THE ASTROPHYSICAL JOURNAL, 304:646–650, 1986 May 15

SIMULTANEOUS SUBMILLIMETER AND INFRARED OBSERVATIONS OF FLAT-SPECTRUM RADIO SOURCES

T. L. ROELLIG[1]
Space Science Division, NASA/Ames Research Center
E. E. BECKLIN
Institute for Astronomy, University of Hawaii
C. D. IMPEY
California Institute of Technology
AND
M. W. WERNER[1]
Space Science Division, NASA/Ames Research Center
Received 1985 September 23; accepted 1985 November 4

ABSTRACT

We present observations of 12 extragalactic nonthermal radio emission sources made at eight wavelengths between 1.25 and 1000 μm, including the important submillimeter wavelength of 350 μm. Nine of the objects were detected at 350 μm, roughly double the number of objects of this type that have previously been detected at this wavelength. The majority of the observations were made within a three-week time span. Our results, combined with other studies, show that these objects generally have flat energy distributions at wavelengths longer than 1 mm that break in most cases between 350 μm and 1 mm. At wavelengths shorter than 1 mm, the energy distributions fall with a rough power-law behavior with a spectral index of ~ -1. For many of the objects, there is a definite break or curvature in the energy distributions at wavelengths near 2.2 μm, with the fluxes falling even more steeply into the near infrared. At the time of the observations, both OJ 287 and 3C 273 were undergoing flares. Our results are generally consistent with the flares propagating out to longer wavelengths with time.
Subject headings: BL Lacertae objects — galaxies: Seyfert — infrared: sources — quasars

I. INTRODUCTION

Radio loud QSOs, BL Lac objects, and other compact extragalactic radio sources have been extensively studied in the radio up to a frequency of 300 GHz ($\lambda = 1$ mm) and in the near infrared through optical spectral regimes (e.g., Ennis, Neugebauer, and Werner 1982; Neugebauer *et al.* 1979; Landau *et al.* 1983). Except for a few isolated objects (Harvey, Wilking, and Joy 1982; Clegg *et al.* 1983; Neugebauer *et al.* 1984; Gear *et al.* 1985), there has been a gap in the measured spectral coverage between these regimes, particularly in the submillimeter. For the purpose of understanding these objects this is an unfortunate situation, since the energy distributions in this frequency region generally change slope from a fairly flat spectral slope in the radio regime to a strongly negative slope in the near-infrared. By pinpointing the nature of this change, one can set constraints on models of the emission region structure of these objects. We began a program of observations to fill in the spectral coverage gap by making measurements in the submillimeter at 350 μm, together with simultaneous continuum measurements at wavelengths of 1.25, 1.65, 2.2, 3.8, 10, and 20 μm and 1 mm. The simultaneity of these observations is important, since many objects of this type have been observed to vary in brightness. We report here results on 11 QSOs and BL Lac objects and the Seyfert galaxy 3C 84.

[1] Visiting astronomer at the Infrared Telescope Facility, which is operated by the University of Hawaii under contract from the National Aeronautics and Space Administration.

II. OBSERVATIONS

The observations reported here were made at three different telescopes. The objects observed were chosen on the basis of a flat spectrum at high radio frequencies and a relatively large flux at 1 mm. It should be emphasized that this is in no way a complete sample of objects. As a quasar sample it is strongly biased toward highly variable and polarized sources. The 1 mm observations were made at the 5 m Hale telescope in 1983 January and March and 1984 January, using the helium-3 1 mm bolometer system described in Roellig and Houck (1983), and at the IRTF 3 m telescope during 1982 November using the helium-4 1 mm bolometer system described in Whitcomb, Hildebrand, and Keene (1980). All the 1 mm observations were made through air masses less than 2. The 350 μm observations were made at the UKIRT 3.7 m telescope and the IRTF during 1982 November and 1983 April using a recently developed helium-3 submillimeter bolometer system similar to that described in Roellig and Houck (1983) and also the helium-4 submillimeter bolometer system described in Whitcomb, Hildebrand, and Keene (1980).

The submillimeter observations were made through a 295–385 μm filter, which isolated the 350 μm atmospheric window, and a focal plane aperture giving a beam of 39″ FWHM on the UKIRT and 48″ on the IRTF. The objects were all observed on more than one night through air masses less than 1.6 in order to reduce possible systematic errors. Standard infrared chopping techniques, with at least one beam diameter chopper throw, were used for background subtraction. For both the 1 mm and sumillimeter observations, the data were reduced

TABLE 1

OBSERVED FLUXES[a]

Object	1.25 μm	1.65 μm	2.2 μm	3.8 μm	10 μm	20 μm	350 μm	1000 μm
3C 84	...	...	...	...	...	...	7.6 ± 0.8[b,c]	19.8 ± 2.0[b,c]
4C 50.11	0.29[d]	0.53[d]	0.66[d]	1.9[d]	<30[d]	...	4.7 ± 1.1[b,c]	2.9 ± 0.6[b,f]
0735+178	9.70	13	17	26	...	...	<1.7	...
OJ 287	53[d]	68[d]	91[d]	150[d]	440[d]	...	1.4 ± 0.5[b]	3.5 ± 0.7[b,f]
	39	52	68	110	280 ± 20	530 ± 125	4.7 ± 0.9	5.0 ± 0.6[e,f]
	...	...	...	...	...	...	...	6.0 ± 1.2[f,g]
W Com	5.4	8.1	10	20.4 ± 1.1	...	...	<2.6	<1.1[e,f]
3C 273	37	54	88	165	480 ± 28	1400 ± 100	24.4 ± 2.7	70 ± 11[f,h]
3C 279	0.81 ± 0.03	1.5	2.2	5.05 ± 0.59	<50	<205	1.8 ± 0.5	3.9 ± 1.0[f,h]
1308+326	8.2	11	16	27	78 ± 10	240 ± 53	1.4 ± 0.5	2.8 ± 1.0[f,h]
3C 345	6.6	11	16	35	110 ± 13	350 ± 76	4.3 ± 0.8	7.4 ± 1.8[f,h]
1749+096	1.8	2.8	3.7	6.3	...	...	<1.5	2.6 ± 0.7[f,h]
1921−293	...	...	...	...	...	...	2.9 ± 0.8	5.6 ± 1.9[f,h]
3C 454.3	...	1.3[d]	2.0[d]	5.2[d]	26[d]	...	2.5 ± 0.8[b,c]	3.7 ± 0.9[b,c]

NOTES.—All upper limits are 3 σ. Errors are included when they exceed 5%, and include statistical, calibrated, and estimated systematic errors. All observations 1983 Mar 29–Apr 2 except as noted; with UKIRT, except as noted.

[a] Fluxes in mJy for 1.25–20 μm observations, in Jy for 350 and 1000 μm ones.

[b] 1982 Nov. 13–15.

[c] IRTF.

[d] 1983 Jan.

[e] 1983 Jan 1–3.

[f] 5 m Hale telescope.

[g] 1984 Jan 19–23.

[h] 1983 Mar 27.

using the techniques outlined in Elias *et al.* (1978), including bandpass and beam size corrections, with the planet Jupiter as the primary standard. The Jovian brightness temperature was taken from Werner *et al.* (1978) and Cunningham *et al.* (1981) as 168 K at 1 mm and 147 K at 350 μm.

The shorter wavelength infrared observations were made using the facility instrumentation at the UKIRT during 1983 January and April. The apertures for these observations were 10″ at 10 and 20 μm and 8″ at the shorter wavelengths, while the chopper throw was 60″. Bright stars from the list of Tokunaga (1984) were used for calibrations at 10 and 20 μm, while standard stars from Elias *et al.* (1982) were used as calibrators at 1.25, 1.65, 2.2, and 3.8 μm. The fluxes adopted for zero magnitude were 1520, 980, 620, 225, 37, and 10 Jy for 1.25, 1.65, 2.2, 3.8, 10, and 20 μm respectively.

III. RESULTS

The multifrequency observational results are presented in Table 1. The errors listed in this table include statistical errors, calibration uncertainties, and, for the 350 μm and 1 mm observations, estimated systematic uncertainties of 10%. Except for the exceptions noted in the table, all of the observations for any one object were made within a three-week time period (within a one-week time period for all the wavelengths except 1 mm). For the objects OJ 287, 3C 279, and 3C 345 we have observations at similar epochs with those reported in Gear *et al.* (1985). Our results are in good agreement with theirs, except at 1 mm, where our results are systematically 30% higher. After extensive cross checking it appears that this is due to a difference in our filtering compared to theirs. The more accurate of the two values has yet to be determined, but in any case this discrepancy does not affect any of the science discussed below.

The multifrequency results for those objects with near-infrared and submillimeter or millimeter measurements simultaneous to within three weeks are shown in a log frequency/log flux plot in Figure 1. With the exception of 4C 50.11, all the sources show monotonically decreasing fluxes from 1 mm to 1.25 μm. In general, the infrared energy distributions are well represented by a power law, $f \propto \nu^{-a}$. For several of the objects the spectral index changes near 2.2 μm. This change is gradual for some of the objects and a rather sharp break for the others. A measure of the change can be obtained by comparing the spectral indices from 1 mm to 2.2 μm with the indices from 2.2 to 1.25 μm. This is done in Table 2 with indices $a(1)$ and $a(2)$ respectively, together with the radio spectral indices from Ennis, Neugebauer, and Werner (1982). For our observed sample objects we find averages of $a(1) = 1.0$ and $a(2) = 1.3$ with sample standard deviations of 0.3 for both averages.

During the time period covered by the observations, both OJ 287 and 3C 273 flared at some wavelengths. Table 3 gives a chronology of the flares at 1 mm, and multifrequency measurements of OJ 287 at different times are listed in three lines in

TABLE 2

DERIVED PARAMETERS

Object	$a(1)$[a]	$a(2)$[a]	a(radio)[a]	s[b]	e[c]
4C 50.11	1.4	1.5	+0.4	3.8	0.18
0735+178	<0.8	1.0	0.0	<2.6	0.25
OJ 287[d]	0.6	1.0	+0.4	2.2	0.25
OJ 287[e]	0.7	1.0	...	2.4	0.25
W Com	1.1	1.5	+0.1	3.2	0.18
3C 279	1.2	1.8	+0.4	3.4	0.16
1308+326	0.8	1.2	−0.1	2.6	0.22
3C 345	1.0	1.6	−0.1	3.0	0.17
1749+096	1.1	1.3	−0.2	3.3	0.20
3C 454.3	1.2	...	+0.2	3.5	...
Mean	1.0 ± 0.3	1.3 ± 0.3	0.1 ± 0.2	3.0 ± 0.5	0.21 ± 0.04

[a] Power-law spectral indices given by $F_\nu \propto \nu^{-a(i)}$, where F_ν is the flux at frequency ν, $a(1)$ is the spectral index from 1 mm to 2.2 μm, $a(2)$ is from 2.2 μm to 1.25 μm, and a(radio) is from 5 GHz to 15 GHz. The a(radio) indices are from Ennis, Neugebauer, and Werner 1982 and Owen *et al.* 1978.

[b] Energy index of the synchrotron particles given by $N(E) \propto E^{-s}$.

[c] Acceleration parameter as defined in the discussion.

[d] Infrared data taken in 1982 Nov.

[e] Infrared data taken in 1983 Mar.

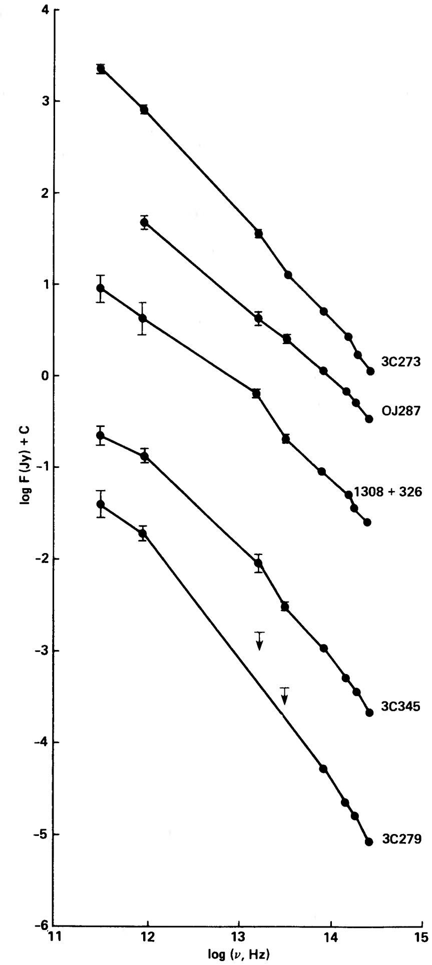

FIG. 1*a*

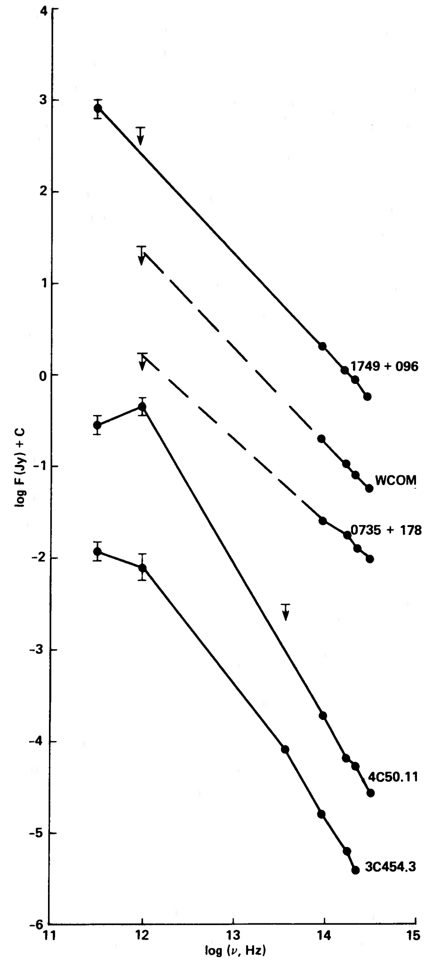

FIG. 1*b*

FIG. 1.—Energy distributions from 1 mm to 1.25 μm for 10 observed objects. The scale constants C, are as follows: 3C 273, 1.5; OJ 287, 1.0; 1308+326; 0.5; 3C 345, −1.5; 3C 279, −2.0; 1749+096, 2.5; W Com, 1.0; 0735+178, 0.0; 4C 50.11, −1.0; 3C 454.3, −2.5. The dashed lines for 0735+178 and W Com indicate that the lines are drawn though an upper limit at the long-wavelength end.

Table 1. The question of short-term variability was briefly addressed by making daily measurements of the submillimeter flux of 3C 273 over a period of a week during 1983 April. We found no changes in the observed flux from this object greater than 10% over the time span.

TABLE 3

ONE-MILLIMETER OBSERVING LOG FOR SOURCES SHOWING EVIDENCE FOR VARIABILITY

Date	Flux Density (Jy)
OJ 287	
1982 Nov 13–15	3.5 ± 0.7
1983 Jan 1	5.0 ± 0.6
1984 Jan 19–23	6.0 ± 1.2
3C 273	
1983 Jan 1	16.7 ± 1.6
1983 Mar 27	69.9 ± 10.6
1984 Jan 19–23	30.0 ± 3.5

IV. DISCUSSION

The most obvious result of our observations is the remarkable similarity in the shape of the energy distributions shown in Figure 1. Our 350 μm results show no evidence for unexpected spectral components in any of the objects. This result is consistent with the results obtained at 100 μm in the publications of Harvey, Wilking, and Joy (1982); Neugebauer *et al.* (1984); and Harvey *et al.* (1984). With the exception of a few objects considered in more detail below, all of the objects have spectral indices of approximately −1 from the submillimeter to 2.2 μm; in many of the objects the slope then curves or steepens to a spectral index of ~ -1.3. A break point at this wavelength has been noted in earlier infrared studies (e.g., O'Dell *et al.* 1978). In addition, comparisons with the results reported in Ennis, Neugebauer, and Werner (1982) show that there is another break point located near 1 mm where the energy distribution steepens from a nearly flat slope in the radio to the observed submillimeter to 2.2 μm slope. Gear *et al.* (1983, 1985) have found that the location of this break point varies from 350 μm to 2 mm depending on the object. We are in agreement with Gear *et al.* (1985) on the location of the break point in the three objects that we have observed in common. The break point also occurs between 350 μm and 1 mm for the balance of our sample.

Any emission model for these objects will have to account for both the break points we have observed. It is clear from the shape of the spectral energy distributions that a standard homogeneous synchrotron source is not a valid model for these sources. A model employing relativistic jets of particles can explain our observed results, but either a transition between two physically different regions, a change in optical depth, or a break in the electron energy spectrum is needed to explain the spectral index changes near 2.2 μm and 1 mm. A possible explanation that would give rise to different regions is an acceleration region within the beam. The published energy distribution for the accelerating beam model of Marscher (1980) is identical in shape with our results, including the correct location of the breakpoints. Although other models can be constructed that are consistent with our results, we will consider here the implications of our results for such an accelerated beam model.

Briefly, these models conjecture an expanding, accelerating, relativistic jet of particles originating from a central energy machine. The observed emission can then arise from four distinct regions. Region I encompasses the central energy machine. Region II is the jet nozzle region, where the particles leave the energy machine and enter the jet. Region III is the acceleration region, where the random turbulent three-dimensional relativistic motions of the particles as they leave the jet are changed into one-dimensional bulk relativisitic flow. In Region IV, the protons are no longer relativistic in their rest frame and the acceleration stops, which freezes the value of the bulk Lorentz factor Γ. This region is then characterized by an expanding, constant-velocity flow. According to this model, as in all relativistic beam models, a compact radio source will be radio loud if the jets are oriented nearly along the line of sight ($\Theta < 1/\Gamma$, where Γ is the bulk relativistic Lorentz factor in Region IV, and Θ is the angle between the axis of the jet and the line of sight). Without the relativistic enhancement caused by the nearly straight-on beaming, a QSO will be radio quiet and have significant emission only from Regions I and II.

We can interpret our results in the framework of this model as follows. The low-frequency flat-spectrum radio emission originates in Region IV, where the source is optically thick. As the frequency increases, the size of the emission region decreases; thus, the observed energy distribution is fairly flat. Eventually, as the frequency increases, one sees far enough into the beam that the transition into Region III is reached.

The 1 mm to 2.2 μm portion of the observed energy distribution originates wholly in Region III, near the transition into Region IV, and has an unmodified synchrotron spectrum boosted in energy by the effects of the relativistic beaming along the line of sight. Contributions from the regions elsewhere in Region III are not seen at these wavelengths because the lower velocity of the bulk flow closer to the energy machine reduces the observed fluxes from these regions. The breakpoint at 1 mm to 350 μm is due to the beam becoming optically thin at the Region III-IV interface, while the 2.2 μm breakpoint is caused by an upper limit to the electron energies in the Region III-IV transition region. The slope in the intervening spectral regime is given by the standard synchrotron formula as $a(1) = (s - 1)/2$, where s is the index in the power-law energy distribution, $N(E) \propto E^{-s}$ of the injected particles.

For the frequency range from 2.2 μm into the optical, the observed emission arises from throughout Region III. The energy distribution is determined by the flow acceleration and the energy loss mechanism for the highest energy electrons in Region III. The effects of the acceleration can be described by a parameter e which defines the jet geometry in the form $r \propto d^e$, where r is the jet cross-sectional radius and d is the distance from the nozzle of the jet. For a nonaccelerating conical jet, $e = 1$; with acceleration in the jet, e is less than 1. When the particle energy loss is dominated by adiabatic expansion losses rather than by synchrotron losses, $a(2) = (1 - e)/3e$ and $e > \frac{1}{6}$. As we see below, this is probably the case for our observed objects.

Using the above model to fit the observed energy distributions from 1.25 μm and 1 mm, and assuming adiabatic losses to be dominant, we derive the values for s and e given in Table 2. We find that the values of e are consistent with adiabatic expansion losses determining the high-energy cutoff for most of our observed sources, although some are very close to the critical value of $\frac{1}{6}$. Assuming synchrotron losses to be dominant does not give consistent values for e.

For the observed objects with sharp break points in the energy distributions near 2.2 μm, the similar frequencies of the observed break points indicate that the quantity $\Gamma\nu_0$ (the product of the bulk Lorentz factor Γ and ν_0, the high-energy cutoff frequency in the transition between Regions III and IV) is constant. The observed location of this break point will be shifted in frequency by the redshift correction factor $1 + Z$, where Z is the redshift of the object. Within the resolution of our data and the range of measured redshifts of our objects ($Z = 0.16$ to $Z = 0.86$, Hewitt and Burbidge 1980), we are unable to see this frequency shift. It is expected that the slope in the near-infrared can be extrapolated into the optical, until the flux from the unmodified synchrotron spectrum of the central energy machine becomes dominant and flattens out the energy distribution.

V. NOTES ON INDIVIDUAL OBJECTS

1. 4C 50.11.—This is the only object observed with a 350 μm flux higher than the 1 mm flux. Within the errors, this implies that the radio spectrum is flat or rises out to 350 μm. The infrared spectrum can be extrapolated smoothly through this point as well, indicating that this may be the location of the break point, rather than at longer wavelengths as in the other objects. A further peculiarity of 4C 50.11 is the lack of any spectral steepening at wavelengths shorter than 2.2 μm.

2. 3C 273.—3C 273 underwent a flare in the infrared through radio during our 1 mm monitoring period (Robson *et al.* 1983). Our 1.25, 1.65, and 2.2 μm observations showed the fluxes at these wavelengths to be at the quiescent levels observed by Neugebauer *et al.* (1979), indicating that the flare had subsided at these wavelengths from the levels reported in Robson *et al.* (1983). Our results at 350 μm and 1 mm are considerably above the quiescent level; this behavior is consistent with the flare originating at shorter wavelengths and then propagating out to longer wavelengths as it subsides in the near-infrared. This is also consistent with the radio results of T. Balonek (private communication) and Robson *et al.* (1983).

3. OJ 287.—This object also underwent a flare during our observations. As can be seen from Tables 1 and 3, the results are also consistent with the flare starting at shorter wavelengths and then propagating out to longer wavelengths.

4. 3C 454.3.—an inspection of the energy distribution for this object shown in Figure 1 reveals that the spectral break points are not as pronounced at the 1 mm and 2.2 μm wavelengths as they are in the other objects. The distribution as a whole shows a pronounced curvature rather than a power-law behavior. A difference in either the emission region geometry or the injection mechanism for this object could cause this curvature.

5. 1921−293.—We were able to detect this object at the two longest wavelengths, 1 mm and 350 μm, but were not able to get near-infrared data. Our 1 mm point is in excellent agreement with Gear *et al.* (1983), but our 350 μm point shows no sign of the inverted slope they reported between 1100 and 800 μm; instead, it falls on a smooth interpolation between their 1 mm point and their 20 μm point. Since our observations were made months later than theirs, it is possible that time variability in the shape of the energy distribution could be responsible for this discrepancy.

VI. CONCLUSIONS

The conclusions to be drawn from our observations of nonthermal extragalactic objects can be briefly summarized as follows:

1. The 350 μm fluxes of the sources can generally be predicted by interpolating between the 1 mm and near-infrared fluxes, with none of the objects showing strong evidence of unexpected components or energy sources.
2. The energy distributions from 1.25 μm to 1 mm can be well fitted by a power-law energy distribution with a change in slope near 2.2 μm for many of the objects.
3. The energy distributions are consistent with an emission model employing expanding accelerating relativistic beams of particles directed nearly along the line of sight.
4. The results for the two objects that were undergoing flares are generally consistent with the flares originating at shorter wavelengths and then propagating out to longer wavelengths.

We would like to thank the staffs of the IRTF, UKIRT, and Mount Palomar observatories for their assistance in the observations. In particular, we would like to thank I. Gatley for his assistance in using the UKIRT. We would also like to thank G. Neugebauer for his support of this program and the use of his lab facilities at Caltech and Roger Hildebrand for the use of some of his instruments at Mauna Kea. Discussions with the Queen Mary College group, especially Ian Robson, have been particularly fruitful.

REFERENCES

Clegg, P. E., *et al.* 1983, *Ap. J.*, **273**, 58.
Cunningham, C. T., Ade, P. A. R., Robson, E. R., Nolt, I. G., and Radostitz, J. V. 1981, *Icarus*, **48**, 127.
Elias, J. H., *et al.* 1978, *Ap. J.*, **220**, 25.
Elias, J. H., Frogel, J. A., Matthews, K., and Neugebauer, G. 1982, *A.J.*, **87**, 1029.
Ennis, D. J., Neugebauer, G., and Werner, M. W. 1982, *Ap. J.*, **262**, 460.
Gear, W. K., Robson, E. I., Ade, P. A. R., Griffin, M. J., Smith, M. G., and Nolt, I. G. 1983, *Nature*, **303**, 46.
Gear, W. K., *et al.* 1985, *Ap. J.*, **291**, 511.
Harvey, P. M., Joy, M., Lester, D. F., and Wilking, B. A. 1984, *Ap. J. (Letters)*, **287**, L9.
Harvey, P. M., Wilking, B. A., and Joy, M., 1982, *Ap. J. (Letters)*, **254**, L29.
Hewitt, A., and Burbidge, G. 1980, *Ap. J. Suppl.*, **43**, 57.
Landau, R., Jones, T. W., Epstein, E. E., Neugebauer, G., Soifer, B. T., Werner, M. W., Puschell, J. J., and Balonek, T. J. 1983, *Ap. J.*, **268**, 68.
Marscher, A. P. 1980, *Ap. J.*, **235**, 386.
Neugebauer, G., Oke, J. B., Becklin, E. E., and Matthews, K. 1979, *Ap. J.*, **230**, 79.
Neugebauer, G., *et al.* 1984, *Ap. J. (Letters)*, **278**, L83.
O'Dell, S. L., Puschell, J. J., Stein, W. A., Owen, F., Porcas, R. W., Mufson, S., Moffett, T. J., and Ulrich, M. H., 1978, *Ap. J.*, **224**, 22.
Owen, F. N., Porcas, R. W., Mufson, S. L., and Moffett, T. J., 1978, *A.J.*, **83**, 685.
Robson, E. I., *et al.* 1983, *Nature*, **305**, 194.
Roellig, T. P. L., and Houck, J. R. 1983, *Internat. J. Infrared and Millimeter Waves* **4**, 299.
Tokunaga, A. T. 1984, *A.J.*, **89**, 172.
Werner, M. W., Neugebauer, G., Houck, J. R., and Hauser, M. G. 1978, *Icarus*, **35**, 289.
Whitcomb, S. E., Hildebrand, R. H., and Keene, J. 1980, *Pub. A.S.P.*, **92**, 863.

E. E. Becklin: Institute for Astronomy, University of Hawaii, 2680 Woodlawn Dr., Honolulu, HI 96822

C. D. Impey: Mailcode 105-24, Department of Astronomy, California Institute of Technology, Pasadena, CA 91125

T. L. Roellig and M. W. Werner: MS: 245-6, NASA Ames Research Center, Moffett Field, CA 94035